

Search for Nonthermal X-ray Emission in the Ophiuchus Galaxy Cluster

Roman A. Krivonos¹*

¹Space Research Institute, Russian Academy of Sciences, Moscow, 117997 Russia

Received July 1, 2022; revised December 2, 2022; accepted December 2, 2022

Abstract — We present the results of our study of the X-ray emission from the Ophiuchus galaxy cluster based on INTEGRAL/IBIS data in the energy range 20 – 120 keV. Our goal is the search for a nonthermal emission component from the cluster. Using the INTEGRAL data over the period of observations 2003–2009, we have constructed the images of the Ophiuchus galaxy cluster in different energy bands from 20 to 120 keV with the extraction of spectral information. We show that in the hard X-ray energy band the source is an extended one with an angular size of $4.9' \pm 0.1'$. Assuming a fixed intracluster gas temperature of 8.5 keV, a power-law component of the possible nonthermal X-ray emission is observed at a 5.5σ significance level, the flux from which is consistent with previous studies. However, in view of the uncertainty in constraining the thermal emission component in the X-ray spectrum at energies above 20 keV, we cannot assert that the nonthermal emission of the cluster has been significantly detected. Based on the fact of a confident detection of the cluster up to 70 keV, we can draw the conclusion only about the possible presence of a nonthermal excess at energies above 60 keV.

Key words: *X-ray emission, galaxy clusters, nonthermal emission, Ophiuchus cluster.*

INTRODUCTION

Most of the galaxies are in gravitationally bound systems-galaxy groups and clusters that can include from a few to a few thousand galaxies. In galaxy clusters the galaxies themselves account for only 1% of the total mass, which is determined mainly by dark matter (90%) and a hot gas (9%) with a temperature of 10^7 – 10^8 K. Owing to plasma bremsstrahlung, galaxy clusters are bright X-ray sources.

Massive clusters are usually formed through the merger of smaller ones and, as a consequence, intracluster-gas-heating shocks emerge. According to theoretical models, relativistic electrons emitting in the X-ray (Miniati, 2003) and visible (Yamazaki & Loeb, 2015) bands through inverse Compton scattering and in the radio band through the synchrotron mechanism (Brunetti & Vazza, 2020) are produced during such mergers as a result of first- and second-order Fermi acceleration. There are also other models that explain the origin of the nonthermal emission in the radio and X-ray bands by the annihilation of dark-matter particles (Marchegiani & Colafrancesco, 2016).

The Ophiuchus galaxy cluster is one of the brightest in the X-ray energy band. The X-ray emission from it was first detected in the early 1980s by Johnston et al. (1980, 1981) based on data from the A-2 instrument onboard the HEAO-1 observatory. This allowed one

to measure the hot gas temperature, $kT = 8 \pm 2$, and to estimate the angular size of the cluster, $R_{\text{Oph}} = 3.9 \pm 1.2$ arcmin (90% significance level). Its redshift $z = 0.028 \pm 0.003$ was also measured from the shift of absorption lines. Wakamatsu & Malkan (1981) independently detected the Ophiuchus cluster in the optical wavelength range using images on photographic plates taken with the Palomar Schmidt telescope. They plotted the dependence of the density of galaxies in the cluster $\rho(r)$ on distance r from the cluster center and found that $\rho(r) \sim (1 + r^2/r_c^2)^{-1}$, where the core radius $r_c = 9.5' \pm 1.5'$. They also showed that the Ophiuchus cluster recedes from the Earth with a velocity $v \sim 7400$ km s⁻¹ and concluded that the cluster is approximately at the same distance from us as the Coma cluster. Hence, the redshift is found to be $z \sim 0.025$, consistent with the result of Johnston et al. (1981).

Based on EXOSAT data, Arnaud et al. (1987) estimated the plasma temperature in the cluster to be $kT = 9.4_{-1.2}^{+1.5}$ and the ion abundance to be $0.26_{-0.13}^{+0.14}$ in solar units (90% significance level). Matsuzawa et al. (1996) fitted the X-ray emission from the cluster by a thermal bremsstrahlung model with two iron lines, K_{α} and K_{β} . Based on data from the gas imaging spectrometer (GIS) onboard the ASCA satellite, they obtained the following emission parameters: $z = 0.031_{-0.007}^{+0.004}$, $kT = 9.7 \pm 0.4$ keV, the iron K_{α} and $K_{\beta} = 6.60 \pm 0.04$ keV and 7.8 ± 0.2 keV, respectively, and the iron abundance 0.24 in solar units. The β -model

*e-mail: krivonos@cosmos.ru

was chosen to fit the gas density distribution in the cluster:

$$n(r) = n_0 \left[1 + \left(\frac{r}{r_c} \right)^2 \right]^{-3\beta/2} \quad (1)$$

where n_0 is the gas density at the cluster center and r is the distance from the cluster center. The following model parameters were obtained: $r_c = 3.8'$, $\beta = 0.62$.

A study of the possible contribution of nonthermal emission to the X-ray spectrum of the Ophiuchus cluster (and other clusters) is greatly complicated by the uncertainty in measuring the thermal emission component of the hot gas, which has a multitemperature structure and contains a central cooling flow. In view of the relatively high cluster temperature, measurements at energies above 10 keV are critically important for constraining the parameters of the cluster gas thermal emission model.

Nevalainen et al. (2004) announced the detection of nonthermal emission from the Ophiuchus cluster based on BeppoSAX data at a 2σ significance level. The plasma temperature in the cluster derived by them is $kT = 9.1^{+0.6}_{-0.5}$ keV. The INTEGRAL gamma-ray observatory gives a unique opportunity to obtain a broadband X-ray spectrum of the Ophiuchus cluster. Based on data from the JEM-X and IBIS/ISGRI instruments onboard this observatory, Eckert et al. (2008) recorded nonthermal emission from the cluster with a $4-6\sigma$ significance. They showed that the cluster is detected with confidence at energies above 20 keV. In addition to this study, Nevalainen et al. (2009) extended the spectral coverage to energies below 10 keV using XMM-Newton data and performed a detailed spatial analysis of the thermal emission from the cluster.

The goal of this paper is to continue the search for nonthermal emission from the Ophiuchus cluster and to constrain its parameters using INTEGRAL data in a wide energy range, from 20 to 120 keV. During the long-term in-orbit operation the characteristics of the INTEGRAL instruments gradually degraded, especially after 2009. More specifically, from 2009 to 2012 the energy resolution of the ISGRI detector deteriorated from 5 to 15 keV, while the lower boundary of the energy range rose from 17 to 23 keV (Caballero et al., 2013). The degradation of the IBIS detector state is evidenced by the observed drop in the count rate from a “standard candle” in X-ray astronomy, the Crab Nebula, by $\sim 20\%$ in the period from 2009 to 2010 (see Fig. 6 in Neronov et al., 2021). This greatly complicates the construction of an average X-ray spectrum over a long time interval. Therefore, in this paper we use the highest-quality IBIS data obtained before 2009. Compared to Eckert et al. (2008), we use not only a larger volume of data (the observational data

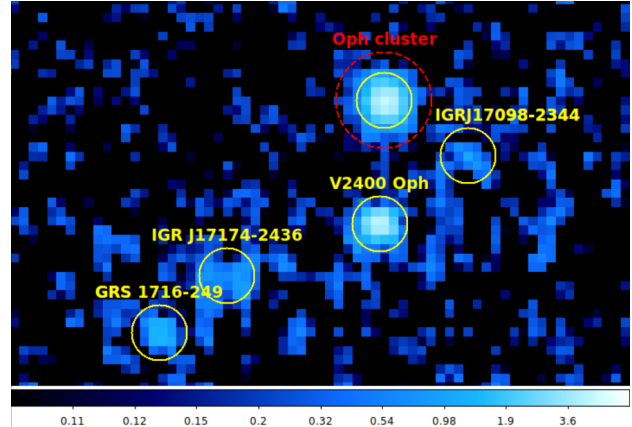


Figure 1. IBIS image of the Ophiuchus galaxy cluster region in the 20–60 keV energy band (in mCrab). The yellow circles mark the positions of the known X-ray sources in the field of view, the circle size corresponds to the angular resolution of the telescope ($12'$). The red dashed circumference indicates the $20'$ region that was used to construct the radial cluster profile. The pixel size is $4'$.

before 2007 were included in Eckert’s study), but also more up-to-date energy calibrations and systematic noise suppression methods in IBIS images (Krivonos et al., 2010).

OBSERVATIONS AND DATA ANALYSIS

The INTEGRAL (INTERnational Gamma-Ray Astrophysics Laboratory) gamma-ray observatory is designed to study cosmic objects in the hard X-ray and gamma-ray bands (Winkler et al., 2003). The observatory is a joint project of the European Space Agency (ESA), Roskosmos, and NASA. It was placed into a highly elliptical geosynchronous orbit in 2002 with a Proton launcher.

In this paper we use data from the IBIS telescope with the working energy range 15 keV – 10 MeV and an angular resolution of $12'$ in a $28^\circ \times 28^\circ$ field of view. The telescope contains two layers of detectors: the upper one, ISGRI, consisting of $4 \times 4 \times 2$ mm CdTe pixels sensitive at energies up to 1 MeV (Lebrun et al., 2003) and the lower one, PICsIT, consisting of $9 \times 9 \times 30$ mm CsI pixels operating at energies above 150 keV.

The IBIS telescope operates on the principle of a coded aperture. Passing through a mask located at some height from the detector, the emission from different sources creates a superposition of shadows (shadowgram) on the detector. The sky image is reconstructed by cross-correlating the shadowgram with the mask transmission function; as a result, an image of the observation region on the celestial sphere is obtained.

The IBIS data were analyzed with the software developed at the Space Research Institute of the Russian Academy of Sciences (see Krivonos et al., 2010, 2012, 2017; Churazov et al., 2014). We constructed the images of the cluster region in several bands from 20 to 120 keV based on the data from 2003 to 2009. The data set being used includes 7367 individual observations of the central part of the Galaxy with an angular shift no more than 15 deg. from the cluster position. The total exposure time is 18 Ms (or, given the dead time, 13Ms). We use the energy calibrations of the INTEGRAL Offline Scientific Analysis (OSA) software of version 10.2.

Angular Size of the Cluster

The X-ray emission from the Ophiuchus galaxy cluster is known to be an extended one with a characteristic size of about 15 arcmin (Nevalainen et al., 2009; Werner et al., 2016), which is comparable to the angular resolution of the IBIS telescope (12 arcmin). Despite the fact that the coded-aperture telescopes are unable to construct the images of extended objects, some information about their angular sizes can still be obtained from the IBIS data (see, e.g., Kuznetsova et al., 2019). In addition, special methods different from those that are used for point sources are required to be applied to properly extract the flux from an extended object. In particular, for the flux from an X-ray source to be correctly estimated, the convolution function, when reconstructing its image, must maximally coincide with the profile of this source for a given telescope.

To determine whether the Ophiuchus cluster is a point or extended source for the IBIS telescope, we investigate the radial cluster flux profile. Figure 1 shows a map of the flux from the Ophiuchus cluster and the X-ray sources nearest to it in the 20–60 keV energy band. To construct the radial profile, we took into account the pixels lying within a circle of radius 20'. At such a distance from the cluster center the intensity drops almost to zero, as can be seen from the radial profile in Fig. 2.

Although the cluster X-ray brightness profile is described by the β -model, to check whether the emission is an extended one, it will suffice to fit the distance dependence of the flux by a Gaussian:

$$I(r) \sim \exp \left(-\ln(2) \frac{r^2}{R^2} \right), \quad (2)$$

where r is the distance from the cluster center and R is the half width at half maximum (HWHM) for the function $I(r)$. In this way we find that $R = 7.7' \pm 0.1'$ ($\chi^2/\text{d.o.f} = 37.7 / 75 = 0.50$). The value of R corresponds to a superposition of the point spread function (PSF) of the IBIS telescope and the radial pro-

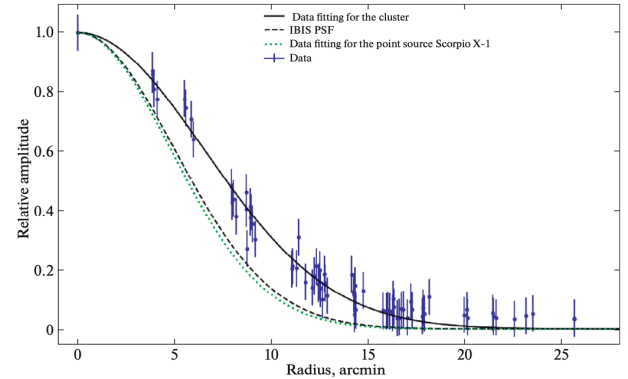


Figure 2. The radial brightness profile of the Ophiuchus cluster in the 20 – 60 keV energy band from ISGRI data (blue dots). The black dashed line indicates the IBIS PSF, the green dotted line indicates the fit to the radial profile of the point source Scorpio X-1. The solid black line indicates the resulting profile from the IBIS PSF and the cluster emission profile. To avoid the coalescence of dots in the figure, we added an artificial scatter of their horizontal coordinates at a $\pm 0.3'$ level.

file of the source: $R^2 = R_{\text{IBIS}}^2 + R_{\text{Oph}}^2$. Hence, knowing the HWHM of the IBIS PSF ($R_{\text{IBIS}} = 5.9'$), we can estimate the HWHM of the source profile: $R_{\text{Oph}} = 4.9' \pm 0.1'$.

Performing similar operations for the point X-ray source Scorpio X-1, we obtain $R_{\text{Sco X-1}} = 5.7' \pm 0.1'$, corresponding to the HWHM of the IBIS PSF: $R_{\text{IBIS}} = 5.9'$ (see Fig. 2). Therefore, this source may be deemed a point one.

Comparing the HWHMs of the radial brightness profiles for the Ophiuchus cluster and the point source, we conclude that the cluster is an extended hard X-ray source. In what follows, the X-ray flux from the cluster will be extracted from the maps convolved with a Gaussian function with $R = 7.7'$, unless stated otherwise.

Model of the Emission from the Cluster

The emission model is a sum of the thermal and nonthermal emissions. The APEC model (see, e.g., Ibaraki et al., 2014) is used for the thermal emission. This model fits the spectrum of a collisionally ionized plasma. It is defined by four parameters: the plasma temperature kT (keV), the redshift z , the normalization $\text{norm}_{\text{apec}}$ (cm^{-5}), and the metal abundance in solar units. The nonthermal emission component is fitted by a power-law model. It includes the following parameters: the exponent α and the normalization norm_{pow} at an energy of 1 keV (photons $\text{keV}^{-1} \text{cm}^{-2} \text{s}^{-1}$).

Thus, there are a total of six unknown parameters. Four of them are fixed from Eckert et al. (2008): the

slope of the power-law model $\alpha = 2$, the abundance of 0.49 in solar units, the temperature $kT = 8.5$ keV, and the redshift $z = 0.028$. These values are consistent with other studies¹ (see, e.g., Matsuzawa et al., 1996; Nevalainen et al., 2004). We will fit the two remaining unknown parameters, the normalizations of both emission components normpow and normappec , from the condition for the minimum of the χ^2 statistic.

Estimation of the Emission Model Parameters

As the fluxes from the cluster and the corresponding errors for each of the energy bands we take the values of the convolved flux maps and their errors at the cluster center.

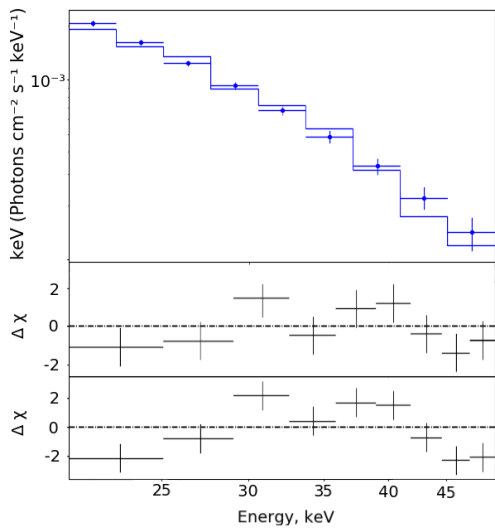


Figure 3. Top: the energy spectrum of the emission from the Ophiuchus cluster from IBIS data in the 20 – 50 keV energy band with errors (blue bins) and the APEC thermal spectral model (blue line). Bottom: the residuals $\{\Delta\chi = (\text{data} - \text{model}) / \text{error}\}$ of the thermal (APEC; top) and power-law (bottom) spectral models.

As a result, the statistic takes a minimum value equal to $\chi^2/\text{d.o.f.} = 1.9$ (d.o.f. corresponds to the number of degrees of freedom) if we set the following values of the parameters being estimated: $\text{normpow} = (3.9 \pm 0.7) \times 10^{-3}$ photons $\text{keV}^{-1} \text{cm}^{-2} \text{s}^{-1}$ and $\text{normappec} = 0.28 \pm 0.01 \text{ cm}^{-5}$. To construct the confidence intervals of both normalizations, we fixed one of these parameters and varied the second one so that the statistic changed by $\delta\chi^2 = 1$. The derived values agree well with previous studies. Our model gives a nonthermal flux of $(6.6 \pm 1.2) \times 10^{-12}$ erg $\text{cm}^{-2} \text{s}^{-1}$ in the 20 – 60 keV energy band. Eckert et al. (2008)

¹ Nevertheless, it should be noted that the assumption about a fixed cluster temperature is a strong one. A mixture of gas phases with temperatures from 1 to 11 keV is known to be present in the central region of the cluster (Werner et al., 2016).

obtained a flux in the 20 – 60 keV energy band of $(8.2 \pm 1.3) \times 10^{-12}$ erg $\text{cm}^{-2} \text{s}^{-1}$, in agreement with our value within the error limits.

DISCUSSION

To check how well the spectrum at energies below 50 keV is described by the thermal law, it was initially fitted by a power law (Fig. 3). A curvature of the residuals is observed, suggesting that the spectrum is thermal in nature. Indeed, if we now model the spectrum by the APEC thermal model (Fig. 3), in which the temperature and the normalization are free parameters, while the remaining two parameters are the same as those in Subsection 2.3, then the reduced chi-squared will decrease compared to the previous case from 3.65 to 1.28.

If we now add the remaining bins with energies above 50 keV to our analysis (Fig. 4, left panel), then the residuals will hardly change. The temperature is determined at a level of ≈ 11.3 keV. Then, we will add a nonthermal component obeying a power law to the model (Fig. 4, right panel). The statistic becomes equal to 1.37. In attempting to construct the confidence interval for the normalization of the nonthermal component normpow , it is possible to obtain only an upper limit on it, which is 2.3×10^{-3} photons $\text{keV}^{-1} \text{cm}^{-2} \text{s}^{-1}$.

Then, we will set the temperature $T = 8.5$ keV, as was done in Eckert et al. (2008). The 1σ confidence interval for normpow in this case is $(3.2 - 4.6) \times 10^{-3}$, giving a 5.5σ detection significance for the nonthermal signal. The statistic becomes equal to $\chi^2/\text{d.o.f.} = 1.9$. The contributions from the thermal and non- thermal emission components in the 20 – 60 keV energy band at this temperature are related as 4:1.

Their total flux in this energy band is $(3.7 \pm 0.25) \times 10^{-11}$ erg $\text{cm}^{-2} \text{s}^{-1}$. The nonthermal flux in this band $(6.6 \pm 1.2) \times 10^{-12}$ erg $\text{cm}^{-2} \text{s}^{-1}$. The nonthermal flux at energies 50 – 70 keV accounts for 5.4% of the total flux in the 20 – 70 keV energy band.

A correlation between the temperature of the thermal component and the normalization of the nonthermal component is also observed: as the temperature rises from 8.5 keV to its optimal value of $T \approx 10.8$ keV, normpow drops from $(3.9 \pm 0.7) \times 10^{-3} \text{ cm}^{-5}$ to $1.3^{+0.9}_{-1.3} \times 10^{-3} \text{ cm}^{-3}$. The correlation is presented in more detail in Fig. 5. Thus, because of the significant uncertainty in the parameters of the thermal emission component in the X-ray spectrum, it is impossible to talk with confidence about a significant detection of nonthermal emission from the cluster. We can make the statement only about the possible presence of a nonthermal excess at energies above 60 keV.

The cluster significance maps in four bands from 20 to 70 keV are presented in Fig. 6. In the 50 – 70 keV

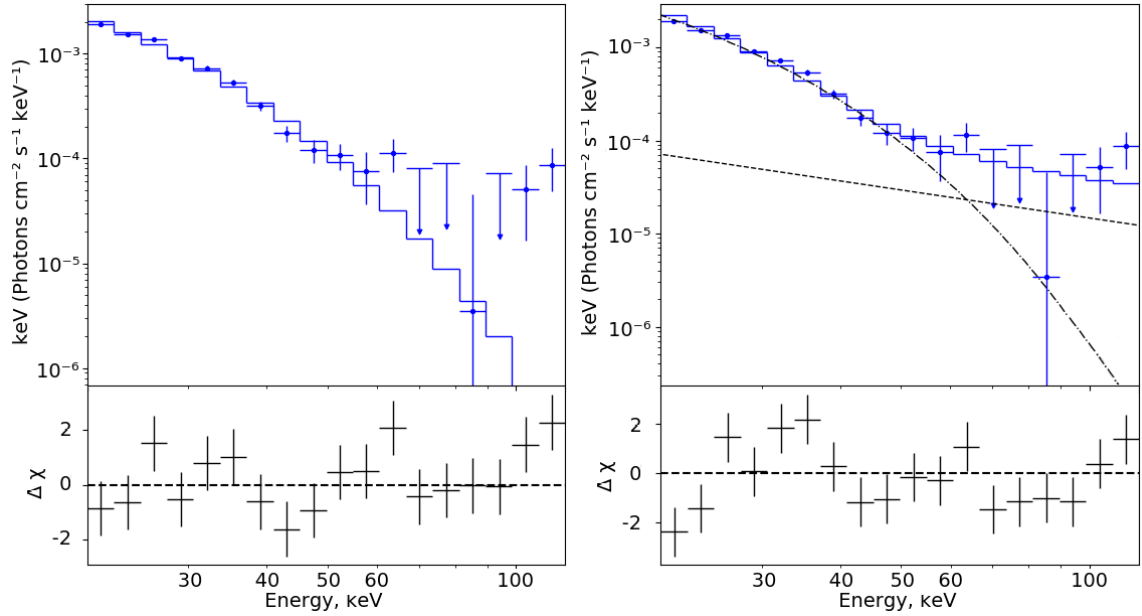


Figure 4. The energy spectrum of the emission from the Ophiuchus cluster from IBIS data in the 20–120 keV energy band. *Top left*: the spectrum was fitted by the APEC thermal model with a temperature of 11.3 keV (blue histogram). *Top right*: the spectrum was fitted by the sum (blue histogram) of the APEC thermal model with a temperature of 10.8 keV (dash-dotted line) and the power-law nonthermal model (dashed line). *Bottom*: the residuals of both models.

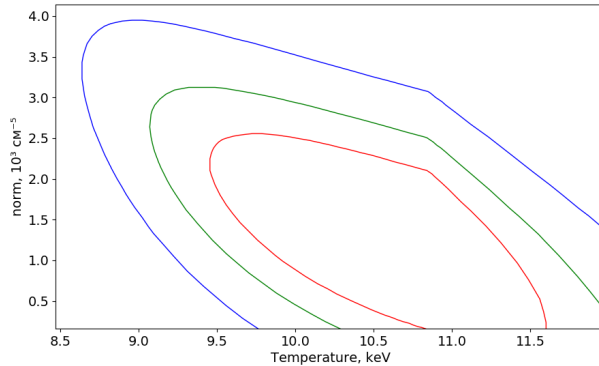


Figure 5. Two-dimensional 1 σ , 2 σ and 3 σ confidence contours (with two free parameters) for the normalization of the nonthermal component and the temperature of the thermal component in the 20–120 keV energy band.

energy band the cluster is observed with a 4.3 σ significance, i.e., we can talk about a significant detection of the cluster at energies up to 70 keV.

CONCLUSIONS

In this paper we presented the results of the observations of the Ophiuchus galaxy cluster with the IBIS telescope onboard the INTEGRAL observatory in a wide energy band, 20–120 keV, based on the observational data from 2003 to 2009. The source was shown to be an extended one in the hard X-ray band.

We demonstrated the presence of an excess nonthermal emission with respect to the thermal one with a fixed temperature of 8.5 keV at a 5.5 σ significance level. In that case, the normalization of the power-law nonthermal emission model is equal to $(6.6 \pm 1.2) \times 10^{-12}$ erg cm⁻² s⁻¹ in the 20–60 keV energy band, consistent with the result of Eckert et al. (2008) within the error limits (see Subsection). However, because of the uncertainty in the parameters of the thermal emission component in the X-ray spectrum at energies above 20 keV, it is impossible to make the statement about a significant detection of nonthermal emission from the cluster. Based on the fact of a confident detection of the cluster up to 70 keV, we can draw only the conclusion about the possible presence of a nonthermal excess at energies above 60 keV. For a confident answer to this question, it is necessary to improve the quality of observations at energies above 60 keV, which can be done using the entire INTEGRAL observational data set. We are planning to do this in our future paper.

On the other hand, it is required to supplement the spectral coverage of the hard energy band by measurements below 10 keV, data from telescopes with a sufficient spatial resolution for a more severe limitation of the multitemperature thermal model of the cluster, for example, as was done in Nevalainen et al. (2009). This will allow one to avoid using the assumption about a fixed cluster temperature. According to Werner et al.

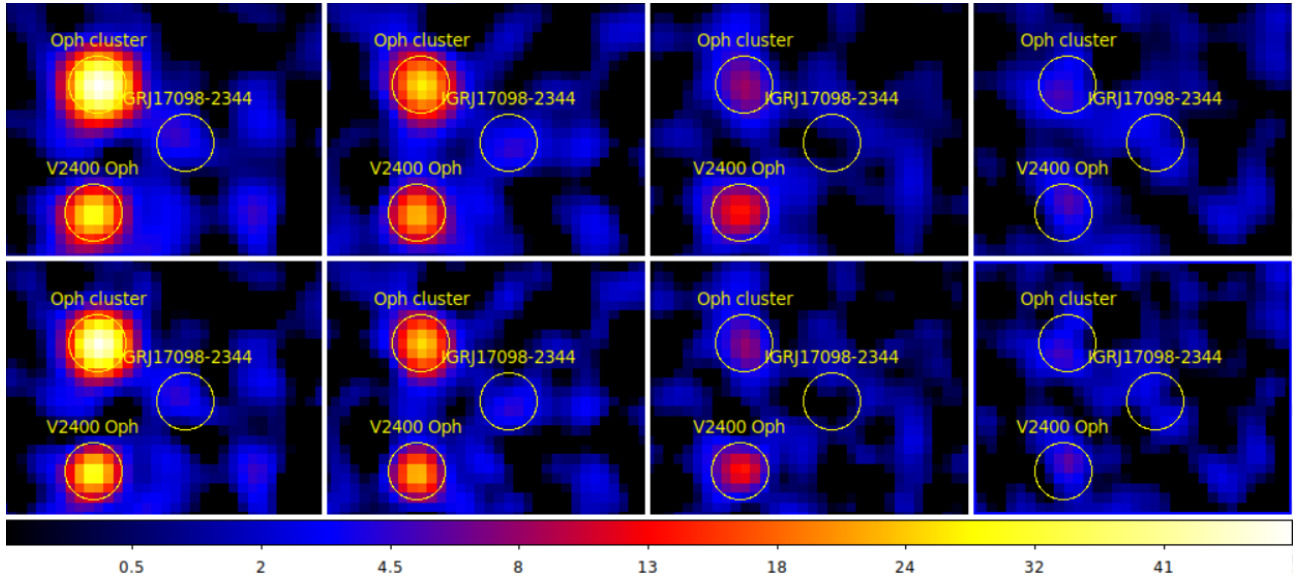


Figure 6. Significance maps of the signal from the Ophiuchus cluster and the sources nearest to it. Four energy bands from left to right are presented in each of the two rows: 20 – 30, 30 – 40, 40 – 50 and 50 – 70 keV, respectively. *Top:* the maps were obtained by convolving the flux maps and their errors with a Gaussian with $R = 7.7'$ (see Subsection). *Bottom:* Similar to the upper row of maps, but for a Gaussian with $R = 5.9'$, corresponding to a point source.

(2016), a hot gas with a temperature up to 11 keV is observed in the Ophiuchus cluster. The emission of a gas with such a temperature will dominate at energies above 20 keV, which is observed in this paper: fitting the X-ray spectrum with a free temperature gives an estimate of about 11 keV (see Section).

However, adding the X-ray data below 10 keV to the IBIS spectrum involves difficulties. Most of the X-ray telescopes have small fields of view, which does not allow a homogeneous study of the entire cluster to be carried out. As a result, the multitemperature thermal emission will be measured only in a specific part of the cluster, whereas the IBIS coded-aperture telescope onboard the INTEGRAL observatory measures the emission from the cluster though entirely, but with an uncertain region of the signal extraction that is determined only by the angular resolution of the telescope ($12'$). A more or less unambiguous correspondence to the measured mixture of spatial different-temperature components in the cluster by the INTEGRAL observatory may be expected when using data from the Mikhail Pavlinsky ART-XC telescope onboard the Spektr-RG observatory, which provides a complete coverage of the cluster and has a sufficiently wide operating energy range, 4 – 30 keV.

ACKNOWLEDGMENTS

I am grateful to S.Yu. Sazonov, A.A. Vikhlinin, and E.M. Churazov for the recommendations to improve the paper. This work is based on observations with IN-

TEGRAL, an ESA project with instruments and the science data centre funded by ESA member states (especially the PI countries: Denmark, France, Germany, Italy, Switzerland, Spain), and Poland, and with the participation of Russia and the USA.

FUNDING

This work was supported by the Russian Science Foundation within scientific project no. 19-12-00396.

CONFLICT OF INTEREST

The authors of this work declare that they have no conflicts of interest.

REFERENCES

1. K. A. Arnaud, R. M. Johnstone, A. C. Fabian, C. S. Crawford, P. E. J. Nulsen, R. A. Shafer, et al., *Mon. Not. R. Astron. Soc.*, **227**, 241 (1987)
2. G. Brunetti and F. Vazza, *Phys. Rev. Letters*, **124**, 051101 (2020)
3. I. Caballero, J. A. Zurita Heras, F. Mattana, S. Soldi, P. Laurent, F. Lebrun, et al., *arXiv e-prints*, p. arXiv:1304.1349 (2013)
4. E. Churazov, R. Sunyaev, J. Isern, J. Knöldlseder, P. Jean, F. Lebrun, et al., *Nature*, **512**, 406 (2014)
5. D. Eckert, N. Produit, S. Paltani, A. Neronov, and T. J. L. Courvoisier, *Astron. Astrophys.*, **479**, 27 (2008)
6. Y. Ibaraki, N. Ota, H. Akamatsu, Y. Y. Zhang, and A. Finoguenov, *Astron. Astrophys.*, **562**, A11 (2014)

7. Джонсон и др. (M. D. Johnston, R. E. Doxsey, F. E. Marshall, and D. A. Schwartz), in *Bulletin of the American Astronomical Society*, Vol. 12, p. 487 (1980)
8. M. D. Johnston, H. V. Bradt, R. E. Doxsey, B. Margon, F. E. Marshall, and D. A. Schwartz, *Astrophys. J.*, **245**, 799 (1981)
9. R. Krivonos, M. Revnivtsev, S. Tsygankov, S. Sazonov, A. Vikhlinin, M. Pavlinsky, et al., *Astron. Astrophys.*, **519**, A107 (2010)
10. R. Krivonos, S. Tsygankov, A. Lutovinov, M. Revnivtsev, E. Churazov, and R. Sunyaev, *Astron. Astrophys.*, **545**, A27 (2012)
11. R. A. Krivonos, S. S. Tsygankov, I. A. Mereminskiy, A. A. Lutovinov, S. Y. Sazonov, and R. A. Sunyaev, *Mon. Not. R. Astron. Soc.*, **470**, 512 (2017)
12. E. Kuznetsova, R. Krivonos, E. Churazov, N. Lyskova, and A. Lutovinov, *Mon. Not. R. Astron. Soc.*, **489**, 1828 (2019)
13. F. Lebrun, J. P. Leray, P. Lavocat, J. Crétolle, M. Arquès, C. Blondel, et al., *Astron. Astrophys.*, **411**, L141 (2003)
14. P. Marchegiani and S. Colafrancesco, *J. of Cosmology and Astroparticle Phys.*, **2016**, 033 (2016)
15. H. Matsuzawa, M. Matsuoka, Y. Ikebe, T. Mihara, and K. Yamashita, *PASJ*, **48**, 565 (1996)
16. F. Miniati, *Mon. Not. R. Astron. Soc.*, **342**, 1009 (2003)
17. A. Neronov, V. Savchenko, A. Tramacere, M. Meharga, C. Ferrigno, and S. Paltani, *Astron. Astrophys.*, **651**, A97 (2021)
18. J. Nevalainen, T. Oosterbroek, M. Bonamente, and S. Colafrancesco, *Astrophys. J.*, **608**, 166 (2004)
19. J. Nevalainen, D. Eckert, J. Kaastra, M. Bonamente, and K. Kettula, *Astron. Astrophys.*, **508**, 1161 (2009)
20. K. I. Wakamatsu and M. A. Malkan, *PASJ*, **33**, 57 (1981)
21. N. Werner, I. Zhuravleva, R. E. A. Canning, S. W. Allen, A. L. King, J. S. Sanders, et al., *Mon. Not. R. Astron. Soc.*, **460**, 2752 (2016)
22. C. Winkler, T. J. L. Courvoisier, G. Di Cocco, N. Gehrels, A. Giménez, S. Grebenev, et al., *Astron. Astrophys.*, **411**, L1 (2003)
23. R. Yamazaki and A. Loeb, *Mon. Not. R. Astron. Soc.*, **453**, 1990 (2015)

Translated by V. Astakhov

Latex style was created by R. Burenin